CLUSTER 2: Nanoscale Building Blocks

Period: March 16, 2006 to March 15, 2007

Coordinators: Moungi Bawendi and Hongkun Park

Moungi Bawendi (Chemistry, MIT)
Federico Capasso (SEAS, Harvard)
Kenneth Crozier (SEAS, Harvard)
Cynthia M. Friend (Chemistry & SEAS, Harvard)
Charles Lieber (Chemistry & SEAS, Harvard)
Eric Mazur (SEAS, Physics, Harvard)
Hongkun Park (Chemistry, Harvard)
Shriram Ramanathan (SEAS, Harvard)

International Collaborator(s): Lars Samuelson (Lund University, Sweden)
Seed Funding: Marco Loncar (SEAS, Harvard)

Number of postdoctoral fellows: 1
Number of graduate students: 5
Number of undergraduate students: 3

Introduction

Tremendous progress has been made in the synthesis of nanoscale structures – nanocrystals, nanowires and nanotubes — that serve as building blocks for new devices and applications. However, many challenges remain. They include the synthesis of nanostructures with well-defined sizes and shapes, the synthesis of new classes of materials, the in-depth characterization of newly developed nanostructures, the rational organization of these nanostructures into complex functional structures, and the fusion of nanoscale building blocks with state-of-the-art processing techniques, including e-beam lithography and focused-ion-beam sculpting, to build novel devices.

The ***Nanoscale Building Blocks*** cluster conducts a broad multidisciplinary, multi-investigator research program that is designed to address these challenges. The proposed research is built upon the participants' expertise in the synthesis and characterization (both experimental and theoretical) of nanostructured materials. At the core of the program is the ***rational synthesis of new classes of nanostructures that exhibit new size-dependent properties*** that are distinct from bulk materials, with an emphasis on heterostructures and nanostructures with unconventional shape, as well as on zero-, one- and two-dimensional nanostructures made from new materials, including metal chalcogenides. The ***incorporation of nanostructures into novel device geometries*** constitutes another important part. These new devices will be tested to characterize the physical and chemical properties of the building blocks and to evaluate their technological applicability. ***Understanding the behavior of these nanoscale building blocks*** through theoretical investigations is an important part of the effort, because it is essential to advance the scientific and technological frontiers.

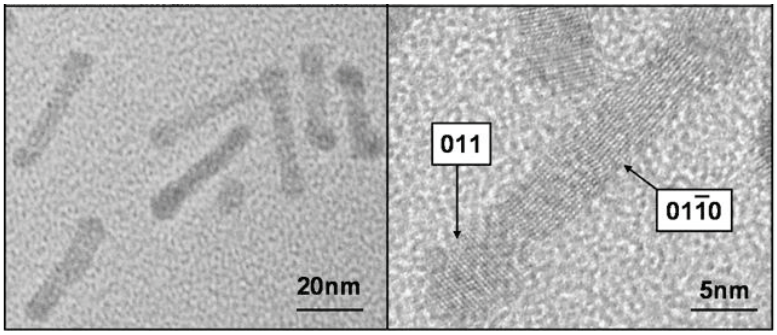

Figure 6.2.0. Electron microscope images of "nanobarbells" specifically made of two semiconductors specifically chosen because electrons are drawn into the "bar" (CdSe) while holes are drawn into the "tips" (CdTe). These could potentially be used in nanocrystal-based solar energy conversion. (**Bawendi**)

Major Accomplishments

Research in the ***Nanoscale Building Blocks*** cluster has made important contributions toward nanoelectronics and nanophotonics in the past year.

The transformation of light into current requires as a first step the rapid dissociation of electrons and holes so that they can be carried to opposite electrodes. This is accomplished in bulk structures by creating an interface between two semiconductor layers that promotes this dissociation. **Moungi Bawendi**'s group has designed and synthesized nano-interfaces in nanocrystal structures specifically to enable the rapid dissociation of electrons and holes at the nanoscale. They have made "nanobarbells" composed of a CdS "ebar" with two CdSe "tips". When illuminated by light, the electrons are drawn into the "bar" and the holes into the "tips". These nano-heterostructures could potentially be used in nanocrystal-based solar energy conversion schemes.

A novel structure of a different type has been made by **Charles Lieber**'s group. They have synthesized p-type//intrinsic//n-type (p-i-n) silicon core//shell//shell nanowires that consist of a single crystalline p-Si core, surrounded by intrinsic Si, then n-Si shells of controlled thickless. Using a selective wet etch, they have separately contacted the p-Si core and the n-Si outer shell. Electrical transport measurements through these show well-defined diode behavior. These new *p-i-n* silicon nanowire structures open up unique opportunities as building blocks for the creation of novel photovoltaics and integrated electronic logic gates.

Federico Capasso and his group have initiated a nanowire optoelectronics program with the goal of developing efficient, room-temperature, electrically-pumped nanowire light emitters, which could form the basis for future integrated photonic circuits. They have developed a novel technique for reliable electrical injection into individual semiconductor nanowires for light-emitting diodes and lasers. In collaboration with **Narayanamurti**, **Capasso**'s group has applied this technique to Gallium Nitride (GaN) nanowires, and have demonstrated ultraviolet electroluminesnce from the GaN band edge. The goal is to produce an efficient nanowire ultraviolet emitter.

A new faculty member in the School of Engineering and Applied Sciences, **Marko Loncar**, was granted seed funding from the Center. He is an expert at making photonic crystals using lithography. **Loncar** is designing hybrid structures that integrate a nanowire inside a photonic cavity to make new types of electro-optical devices.

The challenge of making truly nanoscale devices for future nanoelectronics has inspired research in new materials. **Hongkun Park**, **Shriram Ramanathan** and **Cynthia Friend** are investigating metal-oxide and chalcogenide materials. VO_2 undergoes a metal-insulator (M-I) phase transition that could be used as the basis for a switch.

Hongkun Park has synthesized and tested the properties of VO_2 nanobeams to understand their potential for nanoelectronics. Nanobeams on a substrate experience a coherent uniaxial strain that causes the spontaneous formation of alternating nanoscale metal-insulator domains along the nanobeam length, visualized by **Park**'s group using dark field optical images. The strain produces nanoscale M-I heterostructures within a compositionally homogenous material, and the images demonstrate that VO_2 nanobeams behave as a one-dimensional system for the M-I phase transition.

The Semiconductor Industry Association (SIA) has created the Nanoelectronics Research Institute (NRI) to support academic research to develop quantum switches for ultrasmall electronics in the coming years. Our Center was selected for an NRI supplement for research in new oxide semiconductors that show promise for switches based on metal-insulator phase transitions. This work is carried out by **Shriram Ramanathan**, a new Harvard faculty member from Intel, and by **Venky Narayanamurti**. The potential of new devices for the semiconductor industry is evaluated in the Emerging Research Devices (ERD) panel of the International Technology Roadmap Study (ITRS). **Robert Westervelt** served as part of this panel in 2006, invited by George Bourianoff of Intel.

Lars Samuelson recently joined the Center as an international collaborator. Samuelson is a leading expert in the synthesis of new types of nanoscale structures. He is the Director of the Nanometer Structure Consortium at Lund University in Sweden.

Magnetic and Semiconducting Nanoparticle Systems: Properties and Devices

Moungi G. Bawendi
Chemistry, Massachusetts Institute of Technology
Collaborators: Marc A. Kastner (MIT), George M. Whitesides (Harvard), Robert M. Westervelt (Harvard)

The goal of the research is to use novel nanoparticles, synthesized within the project, in devices that (1) probe the photophysics and transport properties of heterostructures based on the nanoparticles, or (2) use the nanoparticles as building blocks for the design of new optical and electronic devices. We describe here four projects: (1) The characterization of cobalt/cobalt oxide magnetic nanoparticles as a model for coupled ferromagnetic/antiferromagnetic nanoparticle systems, (2) transport properties of CdTe quantum dots in device structures, (3) the synthesis of CdSe/CdTe "nanobarbells" that are designed for efficient carrier separation in photodetectors or solar cells, and (4) the design of layered nanocrystal assemblies for funneling carriers towards electrodes for potential solar energy conversion application.

(1) Magnetic nanoparticle systems and their incorporation into optical structures have been the subject of collaboration between **Bawendi** and **Westervelt**. Previous accomplishments described the synthesis of nanospheres containing both magnetic iron oxide nanoparticles and fluorescent CdSe/ZnS quantum dots. These magnetic/ fluorescent nanospheres could be manipulated using the nanomagnetic manipulator circuits designed by the **Westervelt** group. While this work is still ongoing, here we focus on a careful characterization of Cobalt/Cobalt oxide ferro-magnetic/antiferromagnetic core/shell nano-particles which arose out of our work on designing magnetic/fluorescent particle systems. We found that defects associated with the CoO dominated much of the magnetic behavior of this coupled system. We found that the defect moments freeze at low temperature and have a distribution of melting temperatures. These defects stabilize the magnetic Co core through exchange biasing far above the usual blocking temperature. We also found that switching the biasing field at intermediate temperatures during cooling induced a thermal memory effect, illustrated in Figure 6.2.1, and an opportunity for encoding information.

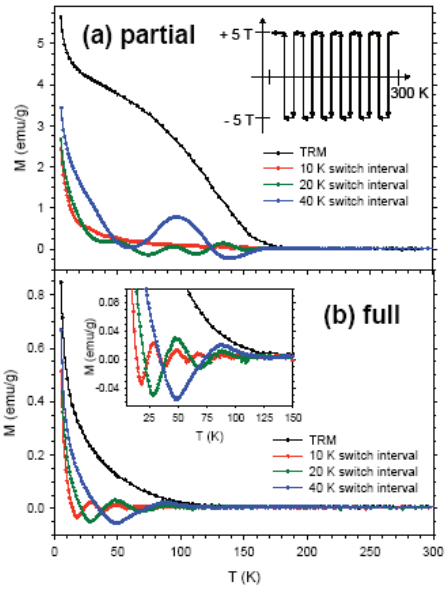

Figure 6.2.1. Magnetization of partially and fully oxidized Co/CoO nanoparticles after cooling from 300 K while switching the magnetic field back and forth at various intervals.

(2) In an ongoing collaboration between **Kastner** and **Bawendi**, we analyzed the details of conduction through nanocrystals of CdTe. We measured the conductance of

close-packed films of CdTe nanocrystals in field-effect structures in the dark and in the presence of light. We found that the majority carriers are holes, that they are injected from gold electrodes into the CdTe nanocrystal films, and that the hole density can be modulated with gate voltage. Secondary photocurrents were found to have a photoconductive gain of ~10 at 10^6 V/cm showing that the hole mobility is higher than the electron mobility. We showed that a single phenomenological description of the field dependence of the hole mobility can explain the dependence of current on source-drain voltage for both dark and light currents.

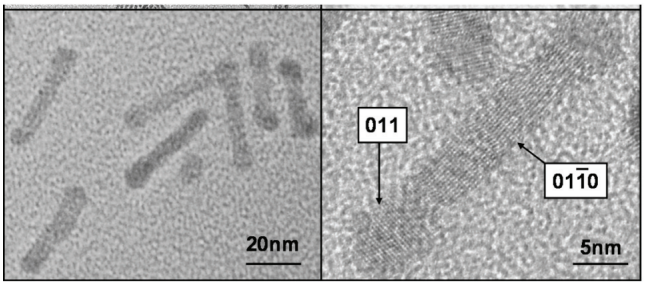

Figure 6.2.2. TEM images of CdSe/CdTe nanobarbells, designed for fast exciton dissociation.

(3) In our goal of designing and synthesizing nanoheterostructures using wet chemical methods, we demonstrated the synthesis of "nanobarbells" consisting of a CdSe nanorod with a CdTe nanocrystal attached at each end (Fig. 6.2.2). This system is interesting for its electronic structure because it is an example of a nanoheterostructures that forms a "type II" system, where an exciton undergoes a fast ionization, with the electron preferring the "bar", and the hole preferring the balls at the tips. This rapid intrinsic carrier separation process is essential to high efficiency nanocrystal based potential solar energy devices. It is the first step in the process of extracting the electron and hole at separate electrodes. We are now in the process of testing the conductive and photoconductive properties of devices based on these nanobarbells to understand their basic transport physics, and how their properties could be used in a solar energy conversion scheme.

(4) Students from **Bawendi**'s group have been collaborating with the **Whitesides** group in designing and characterizing layered nanocrystal structures that are engineered to funnel carriers to the right electrodes in potential solar cell applications. The basic idea is to create a stacked device consisting of an ITO electrode on top of which a series of layers of nanocrystals is deposited, with each layer consisting of smaller particles, and hence with bigger band gaps. By proper choice of the top electrode, directionality is therefore introduced into the device, with the electrons flowing to the ITO, and the holes to the top electrode.

Phase Organization and Oscillation in VO_2 and W-VO_2 Nanobeams

Hongkun Park
Dept. of Chemistry and Chemical Biology and
Dept of Physics, Harvard University
Collaborator: Charles Lieber

First-order solid-solid phase transitions underlie many technologically important material properties, such as ferro-electricity and the metal-insulator transition (MIT). The phase transitions in bulk and thin-film materials occur through heterogeneous domain nucleation and expansion, and materials undergoing repeated phase transitions thus develop complicated domain boundaries and often become polycrystalline. Despite its critical importance in determining the functional characteristics of a material, the dynamics at the domain boundary has been difficult to investigate because domain nucleation and organization cannot be controlled in bulk systems.

In the grant period 2006–2007, we have investigated the combined structural-electronic phase transitions in VO_2 and W-doped VO_2 nanobeams. Specifically, the phase transitions in these nanobeams were studied by incorporating individual nanobeams into a four-probe geometry using electron-beam lithography and measuring their electrical, optical, and scanned probe characteristics. Two distinct types of devices were fabricated: In the first type, an individual VO_2 nanobeam was suspended from the substrate by metal electrodes (suspended devices), whereas in the second type, a nanobeam was lying on a SiO_2 substrate (on-substrate devices).

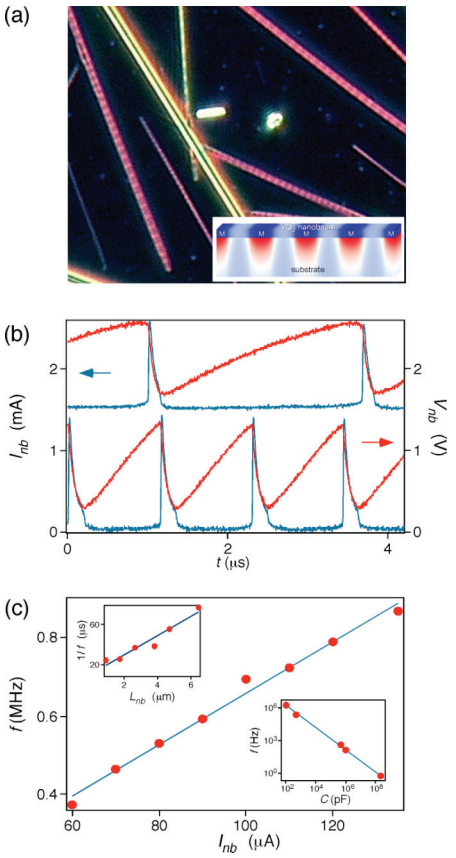

Figure 6.2.3. (**a**) Dark-field optical images of VO_2 nanobeams on a SiO_2 surface (taken at T = 100°C during cooling in air). *Inset*: schematic diagram showing the periodic domain pattern of a VO_2 nanobeam strained on a SiO_2 substrate. (**b**) I_{nb} (blue) and V_{nb} (red) oscillations measured from a $W_{0.01}V_{0.09}O_2$ nanobeam device at two different driving currents. (**c**) f of the electrical oscillation plotted as a function of I_{nb}, with fixed C ~ 150 pF. *Upper inset*: $1/f$ plotted as a function of the nanobeam length (L_{nb}) with I = 28 mA and C ~ 1 nF. *Lower inset*: f as a function of C, with fixed I = 90 mA. The solid lines are linear fits to the data.

Combined electrical, optical, and scanned probe investigations of on-substrate devices reveal that a simple adhesive interaction between the nanobeam and the substrate leads to a coherent uniaxial strain on the nanobeam (Fig. 6.2.3(a)). The resulting strain causes spontaneous formation of alternating nanoscale metal (M)-insulator (I) domains along the nanobeam length, and thus produces nanoscale M-I heterostructures within a compositionally homogenous material [Wu *et al.*, 2006]. This study demonstrates that

VO_2 and W-VO_2 nanobeams behave as a one-dimensional system for M/I domain organization and that the spatial periodicity of M/I domains can be modified by changing the thickness of the nanobeam and the elasticity of the substrate. As such, it suggests a new strategy for strain engineering without the need for epitaxial growth.

Electrical investigation of suspended devices reveals, on the other hand, a phenomenon of current-driven metal (M)-insulator (I) phase oscillations in two terminal devices connected to parallel shunt capacitors [Gu *et al.*, 2006]. The frequency (*f*) of the phase oscillation increases linearly with current, and is inversely proportional to the nanobeam length and the capacitance (C) in the circuit. The maximum *f* of the phase oscillator exceeds 5 MHz for 1-mm long devices when C ~ 100 pF. Analyses of experimental data and theoretical modeling suggest that the phase oscillation, which coincides with the capacitor charging/discharging, is dictated by the Joule-heating-induced M-I transition, heat dissipation, and the Peltier effect and that the phase oscillation occurs through the axial drift of a single M-I domain wall. These observations thus demonstrate that nanobeams and nanowires can act essentially as one-dimensional systems for domain propagation and provide detailed insight into the microscopic mechanism of domain motion. They also demonstrate that the nanoscale MIT might be used to define the electrical oscillator function in nano- and macroelectronic circuits.

Electron microscope characterization and device fabrication were performed using shared facilities at the Harvard Center for Nanoscale Systems.

References

Wu, J., Q. Gu, B. S. Guiton, N.P. de Leon, L. Ouyang, and H. Park, *Nano Lett.* **6**, 2313 (2006).

Gu, Q., A. Falk, J. Wu, L. Ouyang, and H. Park, *Nano Lett.* accepted for publication (2006).

Photonic Systems

Charles M. Lieber
Chemistry and Applied Physics, Harvard
Collaborators: Federico Capasso, Robert M. Westervelt (Harvard)

Lieber and co-workers are developing novel core/shell nanowire building blocks that exploit nanoscale structure-composition modulation to yield specific functional properties. The specific goal of this work is to prepare *p*-type/intrinsic/*n*-type (*p*-*i*-*n*) silicon core/shell/shell nanowire structures that can be utilized to test fundamental limits of photovoltaic conversion in nanoscale structure. To this end, significant progress has been made in several directions including (i) synthetic design, (ii) growth and structural characterization, and (iii) elucidating the basic electrical transport properties. Accomplishments in these three areas are discussed briefly below.

i. Design of *p-i-n* radial core/shell nanowire structures. To synthesize rationally the core/shell nanowires with good control of structure (e.g., core diameter and shell thicknesses) and composition (e.g., independent control of dopant in core and shells), we used the Au-Si binary phase diagram as a guide. Specifically, the single crystal *p*-type silicon nanowire core structure was first elaborated with composition and temperature set within the liquid + solid silicon region (highlighted pink in figure) of the phase diagram using the well-developed metal nanocluster catalyzed vapor-liquid-solid growth process pioneered by **Lieber** and co-workers. To preclude subsequent 1-dimensional elongation when shell growth is desired, the temperature and composition were subsequently changed such that formation of solid silicon–via the vapor-liquid-solid process–is not possible and only homo-geneous growth occurs (highlighted blue in figure). In this way, we can control the initial diameter of the *p*-type silicon nanowire core by the diameter of the nanocluster catalyst, and control independently the thicknesses of the *i*- and *n*-type shells by the temperature and growth time.

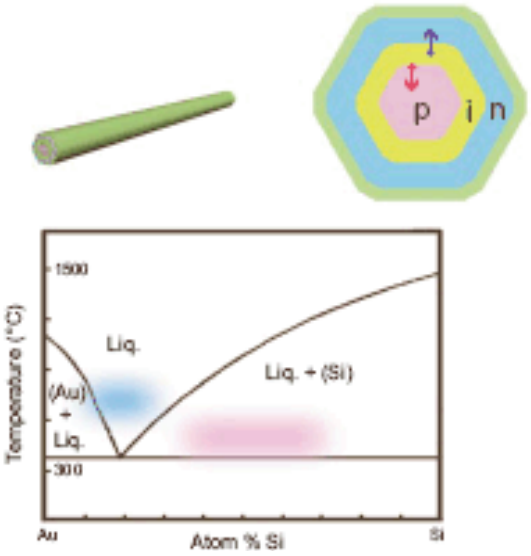

ii. Growth and structural characterization of nanowire building blocks. The p-i-n radial core/shell nanowire structures prepared in this way and fact that the shells are polycrystalline, have been characterized by both scanning electron microscopy (SEM) and transmission electron microscopy (TEM). Representative SEM images of *p-i-n* nanowire structure designed with a relatively thick *i*-layer illustrate clearly the uniform shell growth compared to the single crystalline *p*-type core. A notable advance in this work was the demonstration that imaging contrast of the core/shell structures could be selectively and reproducibly enhanced by using back-scattered electron mode (BSE, lower image) versus secondary electron mode (SE, upper image), where the core appears as lighter at the center region of the structure in BSE mode. This advance enables rapid identification and characterization of the overall quality of the core/shell structure and the diameter of the core and overall sum of the shell

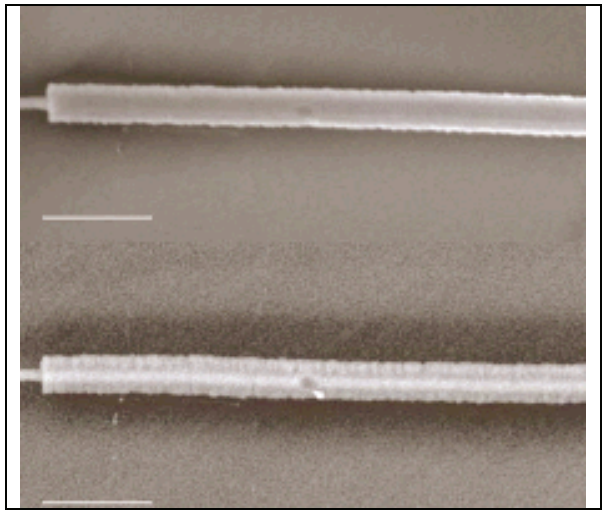

thicknesses. In addition, our TEM studies of the same materials (not shown) confirm the interpretation of the SEM images and provide greater insight into the detailed structures of the polycrystalline shell grains.

iii. Electrical transport properties. We have also made significant progress towards characterization of the electrical properties of these new nanowire building blocks. The initial challenge faced in achieving this goal was the development of a method that would allow for reproducible definition of metal contacts to the core and shell of core/shell nanowires. We overcame this major hurdle by developing the fabrication scheme shown below. First, core shell nanowires are 'pinned' to the substrate using nonreactive metal contact such as chromium. Second, lithography issued to open a window at one end and/or other locations and a selective wet etch is used to remove the *n*-type and *i*-layers are removed. Last, a second lithography and metallization step(s) is used to pattern metal contacts to the core and shell of the nanowire. SEM images show clearly (inset below) that selective etching process can 'expose' the nanowire core selective.

Notably, electrical transport measurements show clearly (a) that we have been able to achieve well-defined diode-like transport for the first time in such nanostructures, and (b) that the fundamental transport properties can be controlled by structure/composition of the shells. Representative data shown below, which was recorded on distinct *p-n* and *p-i-n* structures, show relatively sharp turn-on in forward (positive) bias and rectification in reverse bias. These data demonstrate that the reverse bias leakage can be well-controlled by the *i*-layer, and this variable should provide a critical handle on tuning the properties of these building blocks in subsequent fundamental photovoltaic studies planned for the coming year.

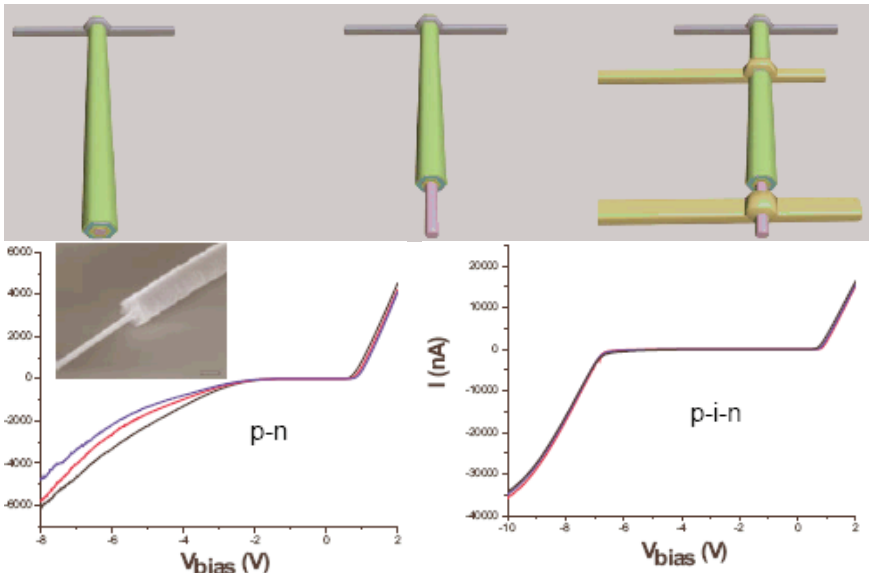

Nanowire Optoelectronics

Federico Capasso
Applied Physics and Electrical Engineering, Harvard University
Collaborators: Venkatesh Narayanamurti (Harvard); Zhifeng Ren (Boston College)

During the last year, **Capasso** and his group have initiated a nanowire optoelectronics program with the goal of developing efficient, room-temperature, electrically-pumped nanowire light emitters, which could form the basis for future integrated photonic circuits. They have developed a novel technique for reliable electrical injection into individual semiconductor nanowires for light-emitting diodes and lasers. Their method

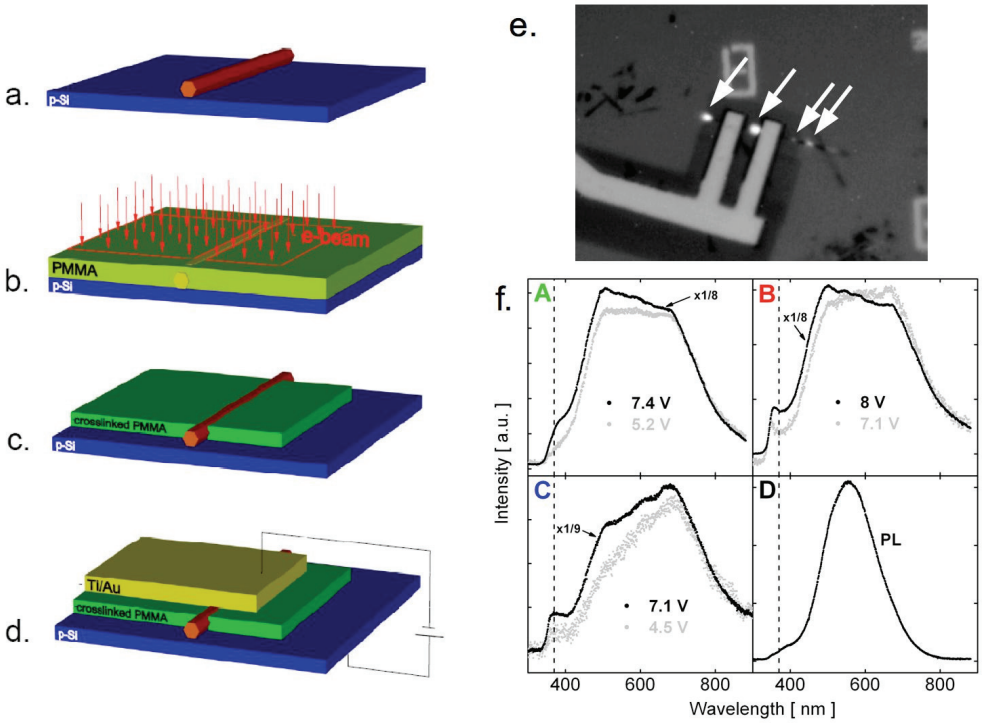

Figure 6.2.4. Schematic description of the procedure to fabricate a single-nanowire LED. (**a**) ZnO nanowires are dispersed on a p-type Silicon (p-Si) substrate (the hole-injecting contact). (**b**) A PMMA thin film (~120 nm) is spin-coated on the substrate. The wire is located and imaged with the SEM of the Focused Ion Beam (FIB) system. The pattern for e-beam exposure is defined directly on the SEM image (red outline), and subsequently written. The dose is ~10 mC/cm^2, which is 15 to 20 times higher than the dose for positive exposure. (**c**) The unexposed and partially exposed PMMA is removed by immersing the sample in acetone. (**d**) Ti/Au is deposited with an electron beam evaporator to form the top metallization. (the electron-injecting contact). (**e**) Grayscale optical image of a single ZnO nanowire LED when a positive voltage (7 V) is applied to the substrate electrode with respect to the metallic contact. The less dark area is the p-Si substrate, and the darkest one is the crosslinked PMMA. The light area is the metallic top contact. The light emission comes from four spots, indicated by the arrows. (**f**) Electroluminescence and photoluminescence spectra of ZnO nanowires at room temperature: (A), (B), and (C) show the electroluminescence of three different LEDs as a function of bias voltage. The higher bias spectra have been scaled by the indicated factor to display them on the same axis as the lower bias spectra. The dashed line indicates the wavelength of band edge emission in bulk ZnO (370 nm). (D) Photoluminescence of a typical single ZnO nanowire.

makes use of a high-resolution negative electron beam resist and direct electron beam patterning for the precise fabrication of a metallic top contact along the length of the nanowire, while a planar substrate is used as a bottom contact. Their technique can be applied to any nanowire structure with arbitrary cross section. They have demonstrated this technique by constructing the first zinc oxide (ZnO) single-nanowire light-emitting diode. The device exhibits broad sub-bandgap emission at room temperature. The material was grown by Prof. Zhifeng Ren and his group at Boston College (Dept. of Physics).

In collaboration with **Venkatesh Narayanamurti** and his group, **Capasso** and his group have applied their technique to Gallium Nitride (GaN) nanowires with the goal of producing an efficient nanowire ultraviolet emitter (Fig. 6.2.5). They have demonstrated ultraviolet electroluminescence from the GaN band edge under *both* bias polarities (Figs. 6.2.5b and 6.2.5c), which they have interpreted as due to tunnel-injection of carriers through thin native oxide barriers.

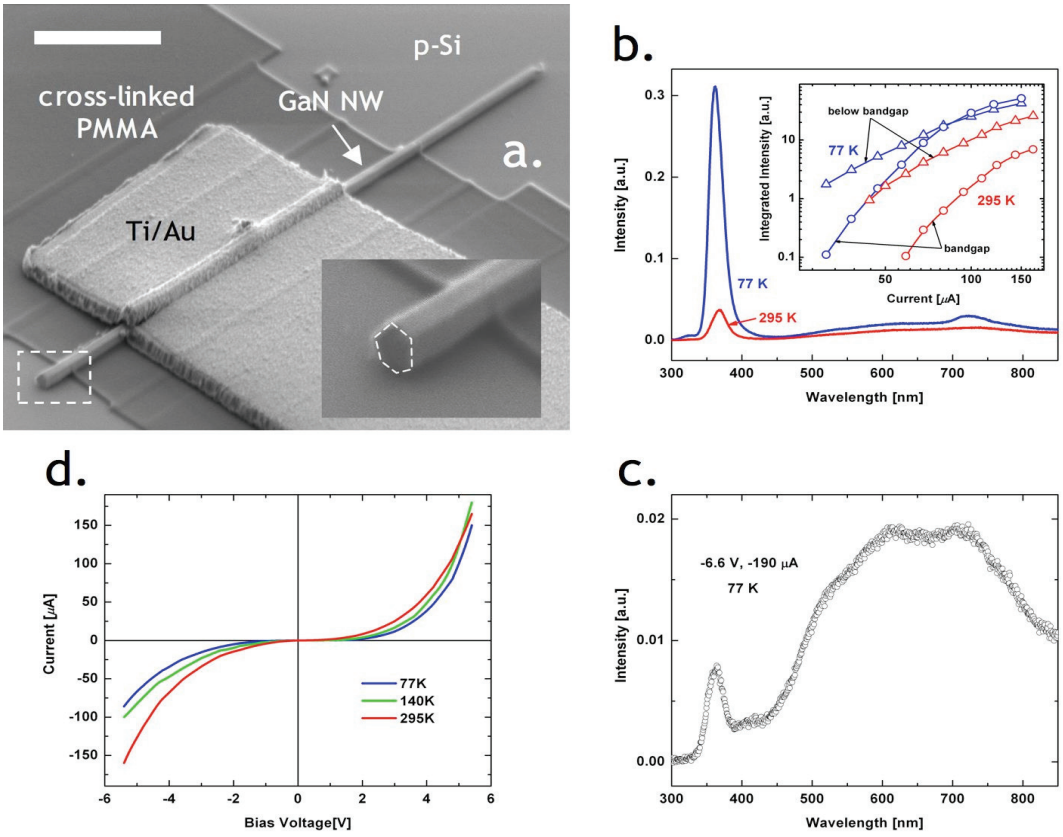

Figure 6.2.5. (**a**) SEM image of single GaN nanowire LED. Scale bar is 2 μm. **Inset**: Zoomed-in image of the nanowire end. (**b**) Forward bias electroluminescence spectra of a typical device at 77 K (blue) and at 295 K (red). Both traces were obtained with the same applied bias of +5.4 V and currents of 150 μA at 77 K and 165 μA at room temperature. **Inset**: Plot of integrated intensity versus current at 77 K (blue) and 295 K (red). The integrated bandgap electroluminescence (open circles) was obtained by adding the measured counts in the range from 300 nm to 450 nm. The below bandgap luminescence (open triangles) was integrated in the range from 450 nm to 850 nm. (**c**) Reverse bias electroluminescence spectrum for single GaN nanowire LED. The a.u. scale is the same in a) and b). (**d**) Current versus voltage characteristics measured at 77 K (blue), 140 K (green) and 295 K (red).

Experimental Measurement of the Dispersion Relations of Gold Nanoparticle Chains

Kenneth B. Crozier
Electrical Engineering, Harvard

Summary. The dispersion relations of plasmon modes of gold nanoparticle chains are measured, and compared with quasistatic theory. In addition to one longitudinal and one transverse mode, the results reveal a third mode, not previously observed.

Research Goal. The miniaturization of optoelectronic circuits to nanoscale dimensions will require waveguides with sub-wavelength lateral mode confinement. This will not be possible with conventional waveguides. An alternative approach, based on chains of metallic nanoparticles, has been proposed [Quinten *et al.*, 1998]. Electromagnetic energy is transmitted along such structures by electrodynamic coupling between the surface plasmon modes of neighboring nanoparticles. As the constituent nanoparticles are only tens of nanometers wide, this presents an opportunity for shrinking waveguides to sub-wavelength lateral dimensions. Theoretical models of the dispersion relations have been proposed [Brongersma *et al.*, 2000; Koendering and Polman, 2006]. However, to the best of our knowledge, experimental measurements of the dispersion relations of metal nanoparticle chains have not been previously reported.

Approach. Gold nanoparticle chains are fabricated on glass slides that are coated with indium tin oxide (ITO) to minimize charging during fabrication. PMMA is spun on and exposed by electron beam lithography. Following development, gold is evaporated to a thickness of 55 nm, with chrome (5 nm) used for adhesion. The PMMA is then dissolved in solvents, with the final result shown below in Figures 6.2.6(a,b). The gold nanoparticle chains occupy a region of 100 μm $\times$ 100 μm. The nanoparticles have diam-

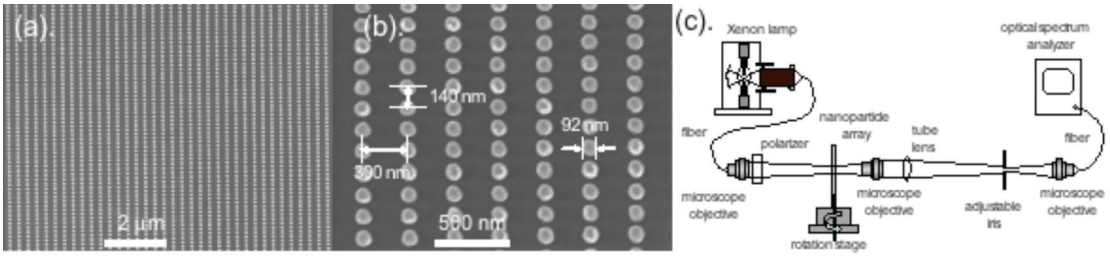

Figure 6.2.6. (a, b). SEMs of gold nanoparticles chains. (**c**) Transmission spectroscopy set-up for measuring dispersion relations.

eters of ~ 92 nm, and center-to-center distances of 140 nm along the length of the chain. Adjacent chains are spaced by 300 nm. Coupling between adjacent chains is expected to have only a minor effect on the dispersion relation, which is expected to be dominated by near-field interactions between neighboring nanoparticles (140 nm spacing).

Transmission spectroscopy of fabricated devices is performed with the set-up shown as Figure 6.2.6(c). Light from a Xenon lamp is focused into an optical fiber. The light from the fiber is collected by a microscope objective, passes through a polarizer and illuminates the sample, which is mounted on a rotation stage. By rotating the sample, the

wavevector k along the nanoparticle chain can be varied, and the resulting plasmon wavelength measured. The light transmitted by the sample is collected by a microscope objective. An adjustable iris is used at the image plane to collect only the light transmitted through the nanoparticle chain array. The light passing through the iris is collected into an optical fiber, and input to an optical spectrum analyzer. The spectrum is then normalized against the spectrum measured through an unpatterned region of the slide.

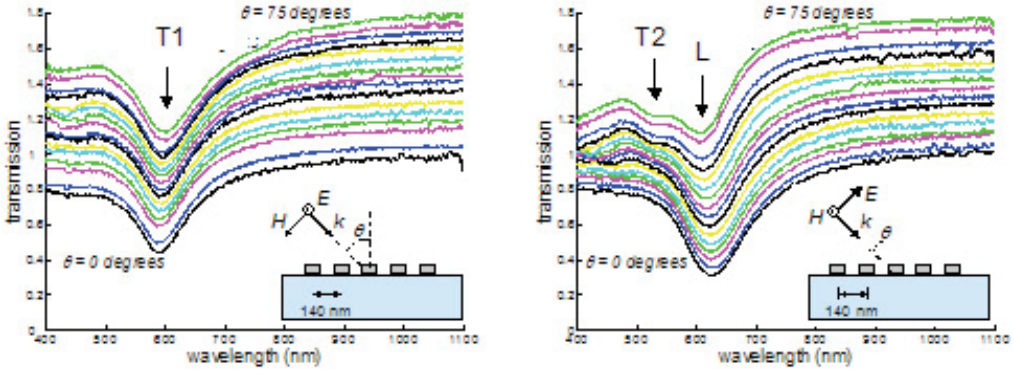

Figure 6.2.7. Transmission vs. wavelength of nanoparticle chains. *Left:* s-polarization. *Right:* p-polarization.

Results and Accomplisments. Transmission spectra are measured with s-polarized (Fig. 6.2.7, left plot) and p-polarized (Fig. 6.2.7, right plot) illumination. The angle of incidence is varied from 0 to 75°, in steps of 5°, and the spectra are vertically offset for clarity. The dips in the spectra correspond to the plasmon resonant wavelengths of the nanoparticle chains. From Figure 6.2.7, it can be seen that s-polarized illumination couples to a single mode (transverse, "T1"). Similarly, p-polarized illumination couples to a single mode (longitudinal, "L") at normal incidence, with an additional mode (transverse, "T2") coupled to at large angles of incidence. The fact that the T2 mode is weaker, only occurs for p-polarized light at high incidence angles and at a higher frequency indicates that this mode is associated with nanoparticle dipole moment oriented perpendicular to the substrate. To the best of our knowledge, mode "T2" has not been previously observed. Previous experimental observations were made either at

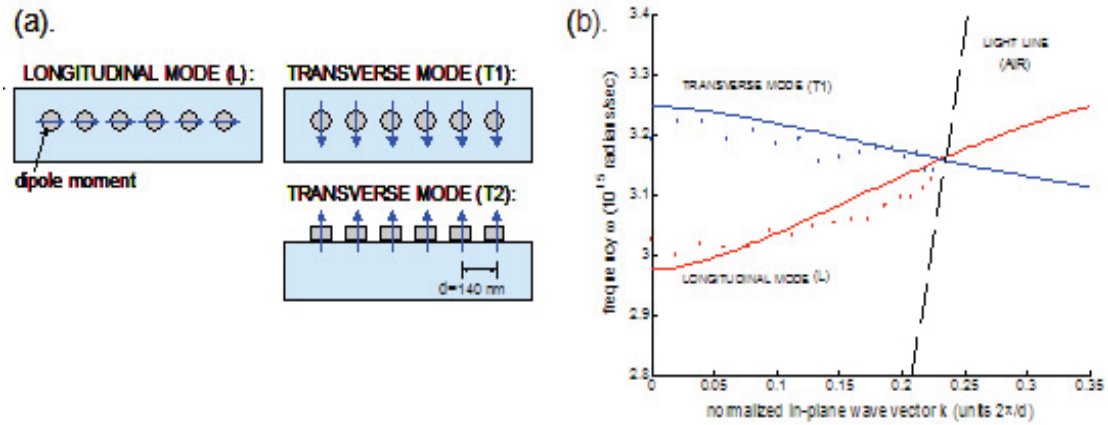

Figure 6.2.8. (**a**) Modes of nanoparticle chains. (**b**) Dispersion relations. Dots: experiment. Lines: theory.

normal [Maier *et al.,* 2002] or 45° [Wei *et al.,* 2004] incidence, and therefore did not excite this mode.

In the longitudinal (transverse) mode (Fig. 6.2.8a), the dipole moments of the nanoparticles are oriented along (perpendicular to) the direction of the chain. The experimental dispersion relations of "L" and "T1" modes are shown as Figure 6.2.8b, with each dot corresponding to a dip in the spectra of Figure 6.2.7. Dispersion relations, calculated using the quasistatic approximation [Brongersma *et al*., 2000; Koenderink *et al.,* 2006] are shown as solid lines in Figure 2.8b. The quasi-static approximation consists of treating the chain of nanoparticles as point dipoles in a uniform medium, with a nearest neighbor near-field ($\sim 1/d^3$) coupling. The dipole moments are found by approximating the nanoparticles as ellipsoids (90 nm $\times$ 90 nm $\times$ 55 nm) in vacuum. The dispersion relations of the "L" and "T1" modes are found, with the only fitting parameter being the plasmon frequency of an isolated nanoparticle. This is found from the plasmon frequencies of the "L" and "T1" modes at normal incidence. It can be seen that the experimental results are in good agreement with theory. We expect that a fully retarded model [Koenderink *et al.,* 2006] will be needed for the accurate modeling of the dispersion under the light line. Additional measurements at larger angles of incidence would allow the dispersion of the "T2" mode to be mapped. The results demonstrate the dispersive nature of metal nanoparticle chains, which will be important for future waveguide applications.

References

Brongersma, M.L., J.W. Hartman, and H.A. Atwater, "Electromagnetic energy transfer and switching in nanoparticles chain arrays below the diffraction limit," *Phys. Rev. B* **62**, R16356–16359 (2000).

Koenderink, A.F. and A. Polman, "Complex response and polariton-like splitting in periodic metal nanoparticles chains," *Phys. Rev. B* **74**, 033,402 (2006).

Maier, S.A., M.L. Brongersma, P.G. Kik, and H.A. Atwater, "Observation of near-field coupling in metal nanoparticles chains using far-field polarization spectroscopy," *Phys. Rev. B* **65,** 193,408 (2002).

Quinten, M., A. Leitner, J.R. Krenn, and F.R. Aussenegg, "Electromagnetic energy transport via linear chains of silver nanoparticles," *Optics Lett.* **23**, 1331–1333 (1998).

Wei, Q.H., K.H. Su, S. Durant, and X. Zhang, "Plasmon resonance of finite one-dimensional Au nanoparticles chains," *Nano Lett.* **4**, 1067–1071 (2004).

Silica Nanowires for Microphotonic Devices

Eric Mazur
Applied Physics and Physics, Harvard University
Collaborator: Federico Capasso (Harvard)

Silica nanowires provide strong mode confinement in a simple cylindrical silica-core/air-cladding geometry, representing a model system for the study of the nonlinear propagation of short pulses inside fibers. We observed supercontinuum generation by femtosecond laser pulses in silica fiber tapers of minimum diameters as small as 90 nm. This research was presented at the Photonics West 2006 Conference and was published in *Optics Express* **14**, 9408–9414 (2006).

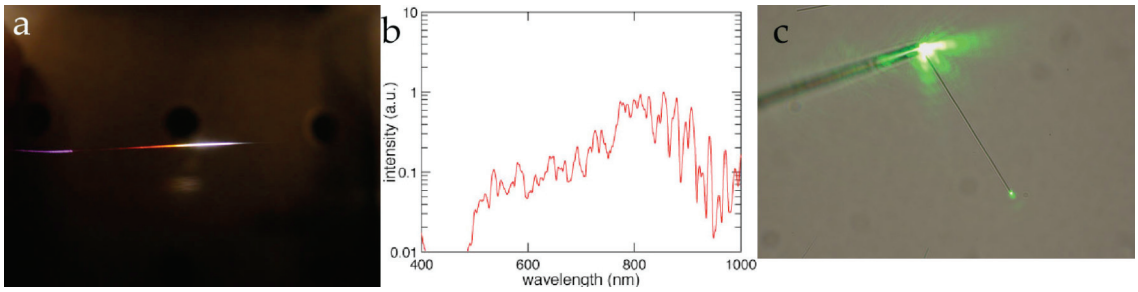

Figure 6.2.9. (a) Photograph and **(b)** spectrum of supercontinuum generation in a 526-nm average diameter silica wire. **(c)** Coupling 532-nm light from a tapered silica fiber into a waveguiding mode of a 60-μm long ZnO nanowire.

Supercontinuum generation refers to extreme spectral broadening of a laser pulse propagating in a nonlinear material. The figure above shows the visual and spectral evidence of supercontinuum generation. Qualitatively, the degree of broadening of the supercontinuum spectra is understood in terms of the diameter-dependent dispersion and nonlinearity of the fiber. Contrary to supercontinuum generation by nanosecond pulses, for laser pulses propagating in negative dispersion regime, the observed spectrum is consistent with higher-order soliton formation and break-up. Because of the reduction of the interaction length to ~20 mm, and the low energy thresholds supercontinuum generation in tapered fibers is a viable solution for coherent white-light source in nanophotonics. Additionally, sub-200-nm diameter fibers possess negligible dispersion and nonlinearity making these fibers ideal media for propagation of intense, short pulses with minimal distortion.

The low threshold energies required to generate supercontinuum indicate that microphotonic devices can be constructed that take advantage of these nonlinear effects. Thus our current research efforts use subwavelength-diameter silica nanowires for the assembly of highly miniaturized photonics devices. Specifically, we plan to manufacture fundamental optical components such as one-to-many splitters, Sagnac interferometers, and nonlinear switches. These components allow efficient parallel assemblies to be produced, significantly reduce the interaction length required for nonlinear phenomena, and create possibilities for optical logic operations and computation. Our efficient and low-cost

technique opens the door to miniaturizing signal-processing nodes to a scale never achieved before.

Silica nanowires have also been used to efficiently launch light into ZnO nanowires, as shown in Figure 6.2.9. The optical properties of semiconductor nanowires are often characterized by using side-illumination. We can directly access the waveguide modes of the semiconducting nanowires by injecting light from tapered silica fibers. Initial results will be presented at the *Photonics West 2007* Conference and a more detailed manuscript describing this research is currently underway.

Synthesis, Imaging, and Electron Transport in 2-D Metal Chalcogenides

Cynthia M. Friend
Chemistry and Applied Physics, Harvard University
Collaborators: Efthimios Kaxiras (Harvard)

During the past year, we have focused on the synthesis and preparation of 2-D semiconductor nanostructures—materials that are 1 atom layer thick—for possible use in mesoscale device structures and as photocatalysts. Very thin and very small structures of semiconducting metal chalcogenides, e.g., MoS_2 and TiS_2, and metal oxides, e.g., MoO_3, are thought to have very different electronic structure than bulk compounds. Furthermore, the electronic properties of these materials are expected to depend on the presence of specific types of defects, especially those related to loss of sulfur or oxygen. To this end, we have also developed methods for introducing vacancies in a controlled manner and subsequently investigating the electronic structure of these materials using density functional theory.

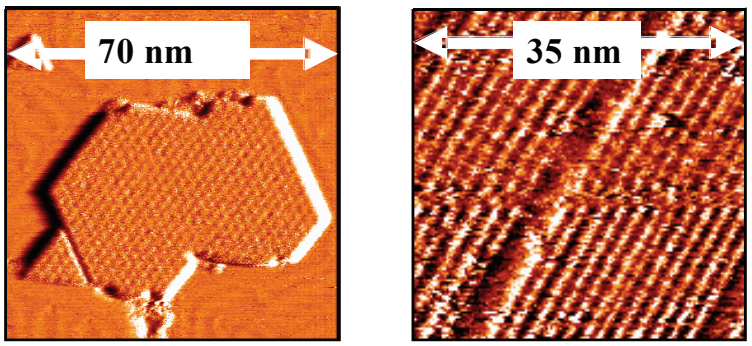

Figure 6.2.10. STM images of stoichiometric TiS_2 nanonstructure (*left*) and reduced TiS_{2-y} showing shear lines due to reduced state (*right*).

We focused on the synthesis of 2-D metal sulfide and metal oxide nanostructures on Au. These materials can, in principle, be transferred to SiO_2 for electronic transport measurements, or studied as possible sensors or catalysts. Our work to date has focused on synthetic approaches and theoretical descriptions of the electronic properties of these nanomaterials. The **Friend** group has already developed a synthetic method for making 2-D metal sulfide nanostructures with well-defined crystalline structure, composition, and morphology. For example, crystalline nanostructures of TiS_2 and MoO_3 have already been synthesized on a Au substrate and imaged using STM [Biener *et al.*, 2005, 2004].

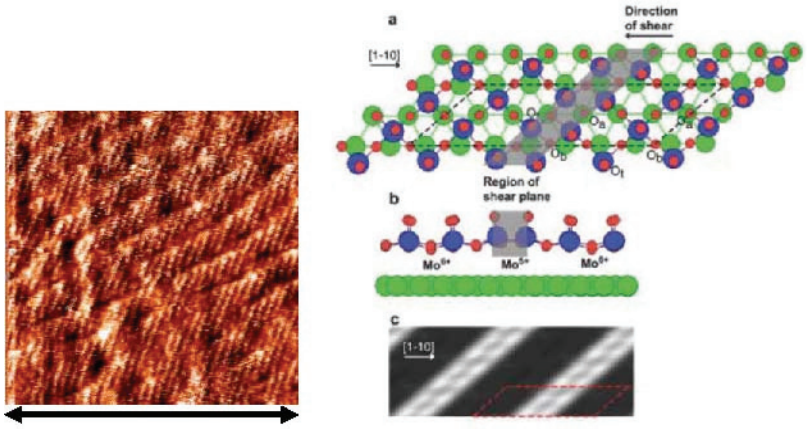

Figure 6.2.11. STM image of reduced MoO_{3-x} nanostructure (*left*) and structure and simulated STM image derived from density functional calculations (*right*).

We have more recently developed methods for controlled thermal reduction of these materials that introduce specific types of vacancies. Both MoO_{3-x} and TiS_{2-y} have been created by synthetic methods developed in our group. In both cases, the nanostructures remain only 1 atom high; however, there are reduced regions of the surface that manifest themselves as shear lines in the STM images (Figures 6.2.10, 6.2.11). Density functional theory was used to study the electronic properties of the MoO_{3-x} and to determine the atomic-scale structure [Quek *et al*. 2006]. The electronic properties of the 1-atom layer high layer is different than the bulk—it is semimetallic. Furthermore, the Mo along the shear lines have a lower oxidation state, indicating that electron transport and chemical reactivity will be different in these regions of the material.

References

Biener, M.M., J. Biener, and C.M. Friend, "Novel synthesis of two-dimensional TiS_2 nanocrystallites on Au(111)," *J. Chem. Phys.* **122** (3), 034,706 (2005).

Biener, M.M., J. Biener, R. Schalek, and C.M. Friend, "Growth of nanocrystalline MoO_3 on Au(111) studied by *in situ* STM," *J. Chem. Phys*. **121** (23), 12010–12016 (2004).

Quek, S.Y., M.M. Biener, J. Biener, J. Bhattacharjee, C.M. Friend, U. Waghmare, and E. Kaxiras, "Structure of incommensurate gold sulphide monolayer on Au(111)," *J. Phys. Chem. B* submitted (2006).

Novel Phenomena in Dioxide Nanostructure

Shriram Ramanathan
Materials (Harvard University)
Collaborators: Venkatesh Narayanamurti (Harvard)

Goal. Use strongly correlated electron systems such as vanadium dioxide which exhibit a metal-insulator transition (MIT) to create novel elementary switching devices with advanced functionality which will hold promise to be employed in the future electronics applications or will advance the understanding of the origin of the MIT in such systems.

Approach. Synthesize high quality vanadium dioxide (VO_2) thin films which exhibit sharp MIT. Perform diverse sample characterization to determine which film growth parameters control the MIT properties. Devise new experiments and device configurations to enhance the switching properties at the MIT and elucidate the origin of the effect.

Accomplishments. RF sputtering of VO_2 target and reactive sputtering of V target in Ar/O_2 environment were used to synthesize pure VO_2 films on Si and Al_2O_3 substrates. X-ray diffraction spectrometry was used to identify the VO_2 phase.

We employed X-ray absorption (XAS) and photoemission spectroscopy (XPS) at the National Synchrotron Light Source of the Brookhaven National Lab to investigate the band structure of the synthesized VO_2 films. Our results can be divided into two parts. First, we found clear changes of the band structure depending on the VO_2 texture and sputtering conditions. This explains at a basic level the observed large MIT properties variation depending on the sample preparation conditions. Secondly, we studied the

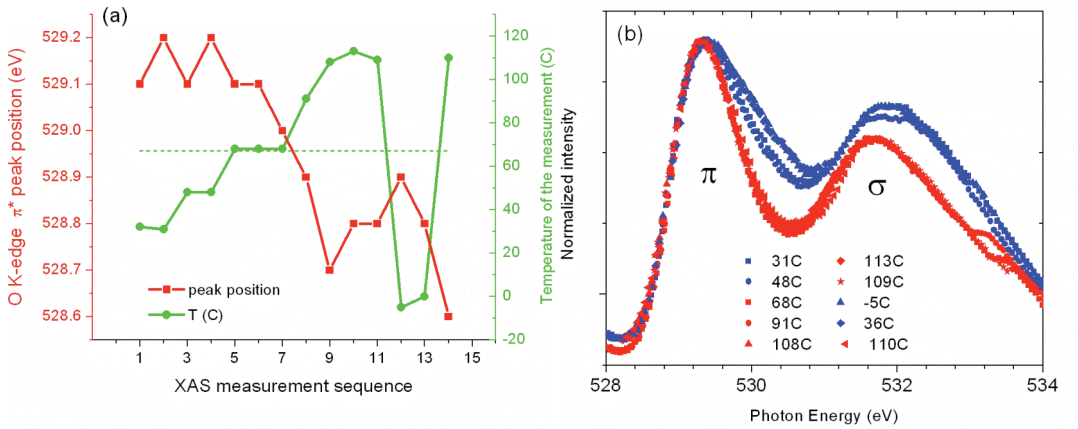

Figure 6.2.12. X-ray absorption spectroscopy analysis of VO_2 thin films across the metal-insulator phase transition boundary. (**a**) The position of the π*-peak in the O K-edge irreversibly shifts toward lower energies upon thermal cycling of the sample. (**b**) O K-edge spectrum at various temperatures. Reversible abrupt switching of π* and σ* bandwidths is observed depending on sample being above (red) or below (blue), MIT temperature (67°C).

temperature dependence of the band structure across the phase transition boundary. We demonstrated for the first time that there were irreversible electronic structure changes happening upon thermal cycling of the sample (Fig. 6.2.12a). This may shed light on the origin of thermal hysteresis in these materials. We also observed reversible π* and σ* band width changes depending on the sample being above or below MIT temperature (Fig. 6.2.12b). These results should enhance the understanding of the origin of the MIT.

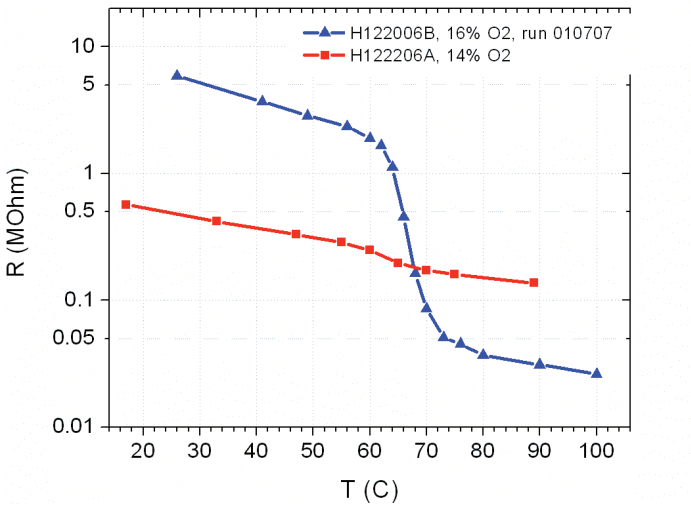

Figure 6.2.13. Resistance dependence on temperature for two samples reactively sputtered in Ar/O_2 environment. MIT is sharper for the sample sputtered in 16% oxygen.

Electrical measurements were performed on the synthesized VO_2 films. The resistance dependence on temperature is shown in Figure 6.2.13 for samples reactively sputtered in 16% and 14% oxygen. The MIT properties are extremely sensitive to the sputtering conditions. Such measurements on VO_2 films allow optimizing the synthesis conditions in order to reliably produce high quality VO_2 with sharp MIT.